Spectrum Analysis of GMA Welter in Various Working Modes

Gökhan Gökmen, Yelda Karatepe

Marmara University Technical Education Faculty, Department of Electricity, Goztepe Campus, Kadıkoy, Istanbul, 34722, Turkey
gokhang@marmara.edu.tr, ykaratepe@marmara.edu.tr

Tahir Çetin Akıncı

Kırklareli University, Engineering Faculty, Department of Electrical and Electronics Engineering, Kavaklı Campus, 39100, Kavaklı, Kırklareli, Turkey
cetinakinci@kirklareli.edu.tr

Memduh Kurtulmuş

Marmara University Technical Education Faculty, Department of Electricity, Goztepe Campus, Kadıkoy, Istanbul, 34722, Turkey
memduhk@marmara.edu.tr

Abstract: In this study, a current drawn by a welter at initial, stable-state and finish modes is examined using spectral analysis. The current shunt measurement method is utilized in order to measure the current drawn by the welter. The study involves the examination of welding stages of a material with the electrode of a welter. First, the current drawn by the welter is measured in the initial mode of the welding process. Then the current value during the stable-state mode of the welding process is measured. Finally, the current drawn at the finishing mode of the welding process is measured. Fast Fourier Transform (FFT) of all these measured current values are calculated and spectral analysis is performed using these transforms. During the study, it is observed that current drawn by the welter during these three modes of welding are different from each other. For each mode, frequency domain analysis of the measured current is performed.

Keywords: Welters; high frequency inverter; working modes; current shunt measurement; spectral analysis

1   Introduction

GMA (Gas Metal Arc) welding is widely used in many industrial applications for metal joining. The GMA welding machine produces an electrical arc between a metal electrode and the weld pool, with shielding from externally supplied gas, which may be an inert, active or a mixture gas. The occurred arc and its heat melts the metal surface and the metal electrode, then molten metal of the electrode is transferred to the work where it becomes the deposited weld metal [1, 2, 3, 4, 5, 6].

All electric arc welding machines work similarly. They dissolve electrodes for connection [8, 9, 10, 11]. In practice, there is a lot of work on the electric arc welding machines [12, 13].

According to the application of power electronics technology, in the GMA welding machine area, higher quality, less spatter generation and more automation are required. These requirements can be met by using the high-frequency inverter arc welding machine that are in this study.

Generally, the GMA Welding Machines widely used in the industrial area can be classified into MIG (Metal Inert Gas), MAG (Metal Active Gas) and GMAW (Gas Metal Arc Welding) welding machine types, according to the utilized shielding gas which prevents oxidizing molten pool or globule. Especially among these GMA welding machines, the CO_2 GMA welding machine is widely used because the price of shielding gas utilized is less expensive. But it has a major disadvantage: it generates more spatter during the welding procedure. The spatter which is generated during welding procedure is the small article radiated to space, nozzle and base metal. So additional work to remove this spatter is needed [14]. The machine with separate wire feeder used in this study is a professional type water-cooled semi-automatic welding machine designed for heavy industry. It is suitable for high quality welding seams for constructional low-carbon and stainless steels, aluminum and their alloys.

It is important to determine the spectral properties of the current signals of welter for current harmonic analysis, the optimization of welding process and time, calculating of the electromagnetic field and the determination of radiation distribution. In this study, the spectral properties of the current signals of welter for each working mode are analyzed respectively.

One of the most effective ways is the current shunt measurement for monitoring, acquiring and measuring applications of currents. It is also suitable for measuring high currents such as the welter primer current.

2   Current Measurement Method

There are basically three methods of monitoring current. Which of these three is used will depend on a number of factors both intrinsic and extrinsic to the application. These requirements may sometimes also be conflicting. Therefore, a careful balancing of requirements to select the optimum method is required. These three basic methods are resistive, optical and magnetic current measurement. The optically isolated resistive method has a medium current range and high isolation, but it has low accuracy and a medium-range cost. Magnetic measurement methods, such as traditional or Hall Effect current transformer, have high current range and medium accuracy, but their cost is very high. The resistive measurement method has high current range and accuracy, and also its cost is very low [15].

In this study, the resistive measurement method was chosen. The measurement of the instantaneous primer current of the welter was carried out by a shunt current measurement. In this method, the current to be measured passes into a resistor and it leads to voltage of shunt resistor. This voltage is proportional to measurement current. The shunt voltage is very low, so it must be amplified by an operational amplifier. A sense resistor must be placed between load and source [16, 17, 18].

As a shunt resistor, the MP2060 (0.005 Ω) power film resistor was preferred [11, 12, 13, 14] and the INA 146 difference amplifier (Burr-Brown Corporation) was chosen as gain amplifier. The connection scheme of the shunt current measurement method is shown Fig. 1 [18, 19, 20, 21].

The calculation of the output voltage of the INA 146 amplifier is given below [18, 19, 20, 21].

$$V_o = I.R_s.[0.1(1 + R_{G2} / R_{G1})] \tag{1}$$

In this equation, V_o represents the output voltage of the amplifier in V, I represents the welding current in A, R_s represents the shunt resistor value in Ω, R_{G1} and R_{G2} represent the gain adjustment resistor in Ω. $[0.1(1 + R_{G2} / R_{G1})]$ refers to the gain value of the amplifier. If R_{G1} is 100 Ω and R_{G2} is 49.9 kΩ, the gain is 50 [6, 7, 10]. The relationship between the welding current and output voltage is given below:
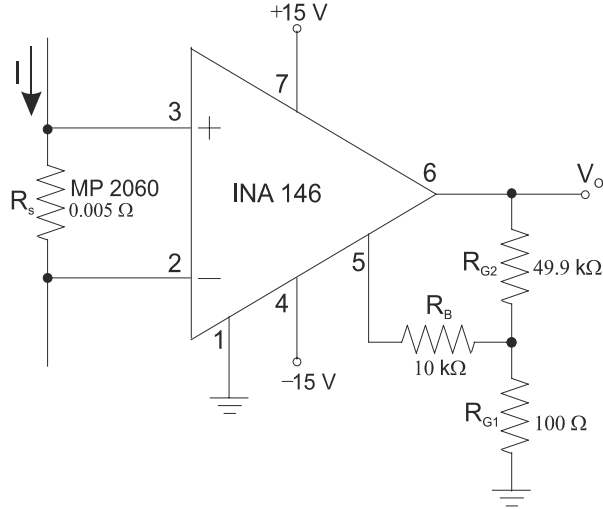
Figure 1
Shunt current measurement [19]

$$I = \frac{V_o}{R_s.[0.1(1 + R_{G2}/R_{G1})]} = 4.V_o \tag{2}$$

If the output voltage is selected $\pm$ 14.475 V (it is almost the maximum amplifier output voltage), the maximum welding current value is calculated as $\pm$57.9 A. This value is accepted as $\pm$1 pu for convenience and subsequent measured current values are specified according to that value [18, 19].

3 Power Spectrum Density

A common approach for getting information about the frequency properties of a random signal is to transform the signal into frequency domain using Discrete Fourier Transform. For data with N-samples, the transformation at $m\Delta f$ frequency is defined as the following equation [18, 22, 23, 24, 25, 26, 27].

$$X(m\Delta f) = \sum_{k=0}^{N-1} x(k\Delta t)^{-j2\pi km/N} \tag{3}$$

In this equation, Δf and Δt represent frequency and resolution at the sampling time, respectively. In this context, specific power spectral density of time series $x(t),$' which is N-sample long, is given as Sxx(f) in Eq. 4.

$$S_{xx}(f) = \frac{1}{N} \left| X(m\Delta f) \right|^2 , f = m\Delta f \tag{4}$$

The cross power spectral density approximation, which is defined between two time series like x(t) and y(t), can be given in a similar way. The statistical accuracy of the approximation given in Eq. 4 increases with the increasing number of discrete data or increasing number of data block containing a sufficient amount of data.

4   Data Acquisition Systems

For data acquisition, a shunt resistor was connected to the primer coil of the welding machine. The output voltage of the amplifier was transmitted to the computer at a sampling rate of 0.005 seconds via an Advantech 1716L Multifunction PCI card, and data analysis was performed using MATLAB-Simulink. This data acquisition system is shown in Fig. 2 [11, 12].
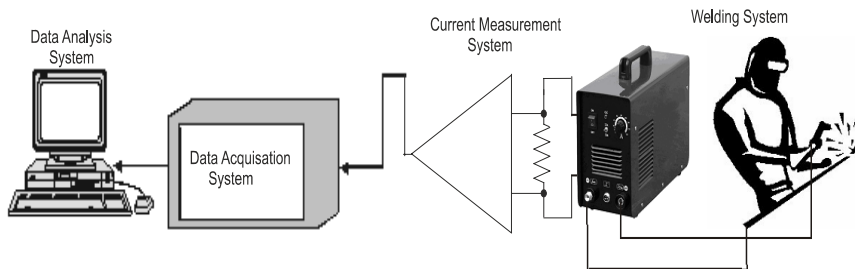

Figure 2
Data acquisition systems [18, 19]

The voltage values of the amplifier are saved separately for three different operation modes of the welding machine. Respectively, these modes are the initial mode, the stable-state mode, which corresponds to the moment reached after a specified time has passed from the starting point, and the finishing mode. As far as these three modes are analyzed, it is seen that the maximum current drawn is 0.92 pu (53.2681 A) and it is drawn at the initial mode. For the other two modes, the peak value of current is observed as 0.6 pu (34.7401 A). The peak current value decreased and is fixed around 0.025 pu (1.44 A) right after the end of the welding [18, 19].

In this study, the welding process is applied to *ST 37* type material by "rutile" basis electrode using the Metal Active Gas (MAG) method. Some specific properties of this welter can be listed as below [18, 19]:

- Frequency: 50/60 Hz

- Number of phases: 3~ AC.

- Primer: 100 VA, Voltage: 440 V-220 V-240 V

- Primer Current: 17/29 A

- Secondary: 55V (DC), 100 %:200 A - 35%: 315 A

5   Data Analysis and Feature Extraction

Data obtained through experimental studies are examined at time-current plane. After the analysis performed, it is observed that the instant alteration of current is composed of high-frequency components. In order to obtain the properties of the high-frequency components, the spectral method is utilized.
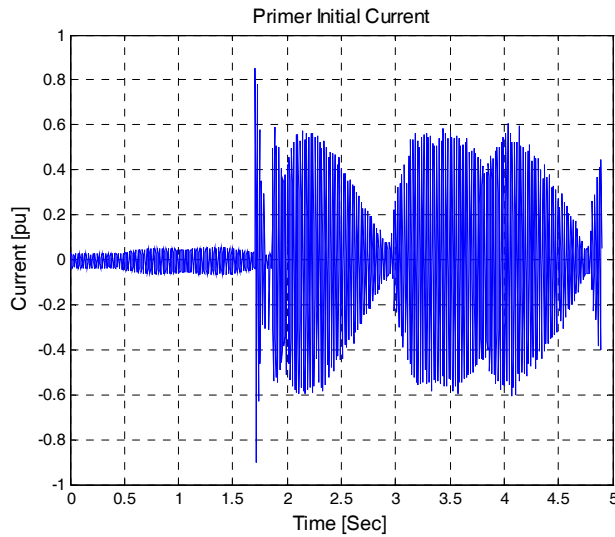

Figure 3
Welding current at the initial mode [13, 14]

In Fig. 3, the current-time graph for the primer current is given. It can be seen that the high current drawn after 1.7 seconds lasts until 3 seconds. At 3 seconds, it drops down to the minimum value and then increases again. When this current-time graph of welding machine is observed, it can be said that it is a characteristic graph for the primer current [18, 19].

When the current-time graph generated for primer initial current of welding machine is expressed at time-frequency plane (Fig. 4), it can be seen that in a frequency band of 45-55 Hz at intervals there are high amplitudes of around 5 seconds. Since mains frequency is 50 Hz, this frequency operation interval can be said to be feasible. In Fig. 4, a high-frequency region is observed at the region labeled as 1 between 1.5-2.2 seconds. This region corresponds to the high current arising after 1.7 seconds at current-time graph. Moreover, high frequency regions are also observed in regions labeled as 2 and 3. These regions are related to the instants when high currents are drawn, as can be observed from current-time graph.
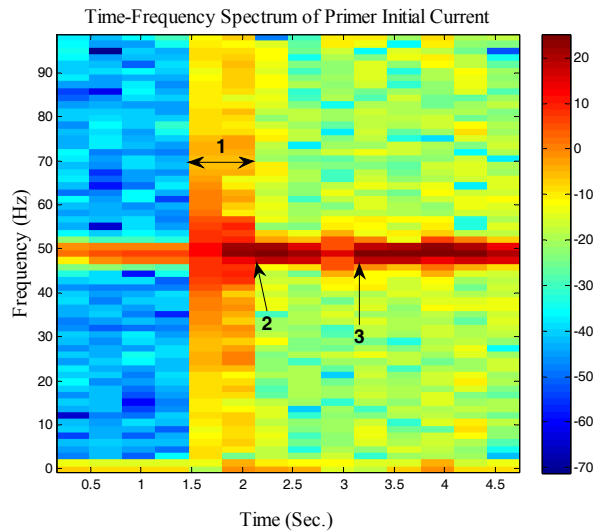
Time-Frequency Spectrum of Primer Initial Current

Figure 4

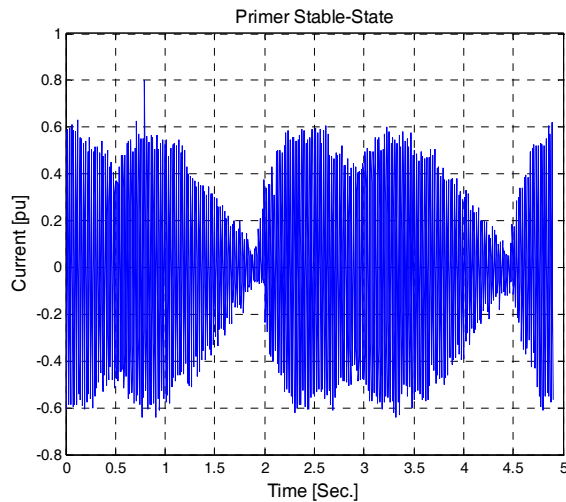Time- Frequency spectrum of primer initial current

Primer Stable-State

Figure 5

Current-Time graph of stable-state mode

The primer current for stable-state instant is depicted in Fig. 5. Here, high current can be observed starting from the starting instant. Even though it decreases at 1.7 seconds, it exhibits an increasing characteristic from that point on. When this current-time graph of the welding machine is observed, it can be said that it is a characteristic graph for the primer stable- state mode.

When the current-time graph generated for primer initial current of welding machine is expressed at time-frequency plane (Fig. 6).
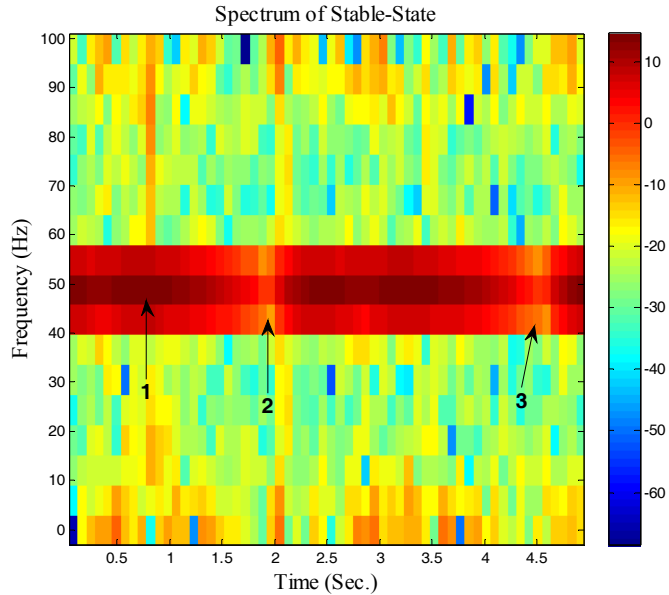

Figure 6

Time-Frequency spectrum of finish-mode

it can be seen that in a frequency band of 45-55 Hz, at intervals there are high amplitudes of around 5 seconds. Here, the region labeled as 1 shows the region at which the welding machine generates the first stable arc. Moreover, this part is the part that builds up the high frequency components. This area corresponds to 10's scale at the color bar on the graph. At the region labeled as 2, there is a lower frequency region between 1.5-2 seconds. It can be seen that the region labeled as 3 is the region at which low arcs occur; low frequency and current are drawn. Lower currents are drawn at regions labeled as 2 and 3 when compared to the region labeled as 1.

In Fig. 7, the current-time graph, which is damped at 0.5 seconds and exhibits an increasing characteristic until 3 seconds, is depicted. This characteristic can be shown as the finish-mode characteristic of the welding machine. In this study, it is observed that the welding machine draws high currents until 2.9 seconds and then it does not perform the welding operation until 5 seconds.
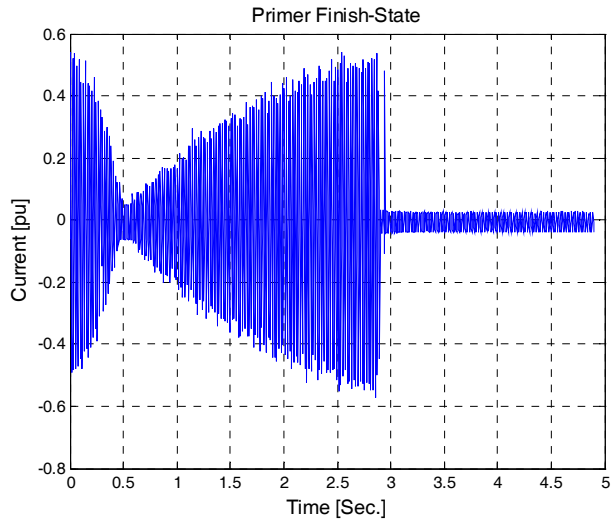
Primer Finish-State

Figure 7
Current-time graph of finish-mode
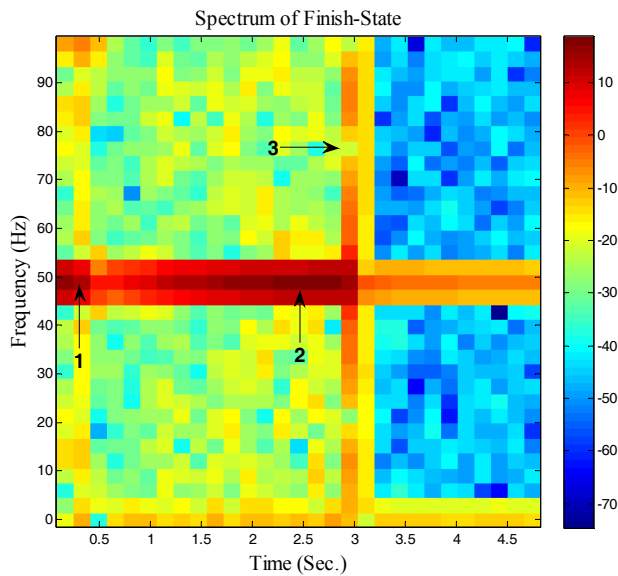
Spectrum of Finish-State

Figure 8
Time-Frequency spectrum of finish-mode

In Fig. 8, the spectrum graph of the Finish mode, which belongs to the current-time graph shown in Fig. 7, is depicted. As can be seen from the spectrum, while region 1 and 2 can be expressed with high-frequency components, region 3 can be expressed with low-frequency components.

Conclusions

In this study, a data acquisition system utilizing a current shunt measurement method for the measurement of the current drawn by welding machine is used, and the data acquired is analyzed using the MATLAB-Simulink package program. After the analysis, the current characteristics of the initial, stable-state and finish modes are determined and the time-frequency spectrums of these characteristics are analyzed.

The extraction of the properties of currents drawn by the welding machine at initial, stable-state and finish modes and performing their spectral analysis are used to specify the current-frequency properties for these different modes. The findings of the analysis result show that the device has a frequency around the fundamental frequency of 50 Hz. In this study on the electric arc welding machine, the spectral analysis method, the source initial mode, operating mode and ending mode frequencies are determined. In addition, this also raises the properties of the different modes. The acquired information contains meaningful results related to the operation states of the welding machine.

References

[1] Correia, D. S., Gonçalves, C. V., Sebastião S. C., Ferraresi V. A: GMAW Welding Optimization Using Genetic Algorithms, Journal of the Brazilian Society of Mechanical Sciences and Engineering, Vol. 26, No. 1, pp. 28-33, 2004

[2] Deruntz, B: Assessing the Benefits of Surface Tension Transfer Welding to Industry, Journal of Industrial Technology, Vol. 19, No. 4, August 2003

[3] Jones, L. A., Eagar, T. W., Lang, J. H: Metal Transfer Control in gas Metal Arc Welding, Tenth Symposium on Energy Engineering Sciences-Argonne National Laboratory, Argonne, IL, May 1992

[4] Funderburk, R. S: Key Concepts in Welding Engineering´-Welding Innovation, Vol. 16, No. 1 and 2, 1999

[5] O'Brien, R: Welding Handbook, Welding Processes. 8th Edition, Miami: American Welding Society, ISBN 0-87171, pp. 110-116, 1991

[6] Ravisankar, V, Balasubramanian, V., Muralidharan, C: Selection of Welding Process to Fabricate Butt Joints of High Strength Aluminum Alloys Using Analytic Hierarchic Process, Science Direct, Material & Design. Vol. 27, No. 5, pp. 373-380, 2006

[7] Ruth, K: Welding Basics: An Introduction to Practical & Ornamental Welding- Creative Publishing International Inc. Minnesota, ISBN 1-58923-139-2, pp. 7-11, 2004

[8] Lancaster, J. F: The Physics of Welding, Phys. Technology, Vol. 15, pp. 73-79, 1984

[9]   http://www.ehow.com/a   bout_4661176_electric-welding-machines.html.
        access date 15.06.2010.

[10]   Palanco, S., Klassen, M., Skupin, J: Spectroscopic Diagnostics on CW-
        Laser Welding Plasmas of Alumi-Num Alloys, Spectrochim - Acta B, At.
        Spectrosc., Vol. 56, No. 6, pp. 651-659, Jun. 2001

[11]   Karabegović, I, Hrnjica, B: Simulation of Industrial Robots for Laser
        Welding of Load Bearing Construction. -Mechanika. -Kaunas:
        Technologija, Nr. 2(76), pp. 50-54, 2009

[12]   Harry, J. E: Measurement of Electrical Parameter of ac Arcs- IEEE
        Transactions on Industry and General Ap-plications, Vol. IGA-5, No. 5, pp.
        624-632, September/October 1969

[13]   Hao, X., Song, G: Spectral Analysis of The Plasma in Low-Power
        Laser/Arc Hybrid Welding of Magnesium Alloy- IEEE Transactions on
        Plasma Science, Vol. 37, Issue 1, pp. 76-82, 2009

[14]   Lanchester, L: The Physics of Welding, 2nd ed. Pergamon Press, ISBN: 13
        978-0080340760, pp. 340, 1986

[15]   Bode, P. T: AN39 Current Measurement Applications Handbook, ZETEX
        Semiconductors, Application Notes, Issue 5, pp. 1-42, 2008

[16]   http://focus.ti.com/analog/docs/mirosite.tsp?sectionId=560
        microsite.tsp?sectionId=560&tabId=2182&micrositeId=7,   access   date
        15.06.2010.

[17]   Koon, W: Current Sensing for Energy Metering, Technical Article, Analog
        Devices, Inc., pp. 2-9, 2010

[18]   Akinci, T. C: Time-Frequency Analysis of the Current Measurement by
        Hall Effect Sensors Electric Arc Welding Machine. Mechanika, ISBN:
        1392-1207, Vol. 5, No. 85, pp. 66-70, 2010

[19]   Akıncı T. C, Nogay H. S, Gokmen G: Determination of Optimum
        Operation Cases in Arc Welding Machine Using Neural Network, Journal
        of Mechanical Science and Technology, Vol. 25, No. 4, pp. 1003-1010,
        2011

[20]   Caddock Electronics, Inc: MP2060 Kool-Pak Clip Mount Power Film
        Resistor, Data Sheet 28_IL128.1004, p. 1, 2004

[21]   Texas Instruments: INA199A1-A3EVM, User's Guide SBOU085, pp. 4-
        11, 2010

[22]   Burr-Brown Corporation: INA146 High-Voltage, Programmable Gain
        Difference Amplifier, Data Sheet PDS-1491A, pp. 1-11, 1999

[23]   Vaseghi, S. V: Advanced Signal Processing and Digital Noise Reduction,
        3rd ed. John Wiley & Sons Inc, ISBN: 0-470-09494-X, p. 449, 2006

[24]   Seker, S: Determination of Air-Gap Eccentricity in Electric Motors Using Coherence Analysis, IEEE Power Engineering Review, Vol. 20, No. 7, pp. 48-50, 2000

[25]   Taskin, S., Seker, S., Karahan, M., Akinci, T. C: Spectral Analysis for Current and Temperature Measurements in Power Cables- Electric Power Components and Systems, Vol. 37, Issue 7, pp. 415-426, April 2009

[26]   Dutoit, T., Marques, F: Applied Signal Processing- A Matlab-based Proof of Concept, Springer Science +Business Media, ISBN: 978-0-387-74534-3, pp. 149-179, 2009

[27]   Arfib, D., Keiler, F., Zölzer, U: Time Frequency Processing. In: DAFX:Digital Audio Effects U. Zölzer, Ed. Hoboken (NJ), John Wiley & Sons, 2002